Journal of Intelligent Manufacturing (2023) 34:515–527
https://doi.org/10.1007/s10845-021-01802-2

A novel parallel classification network for classifying three-dimensional surface with point cloud data

Chen Zhao[1] · Shichang Du[1] · Jun Lv[2] · Yafei Deng[1] · Guilong Li[1]

Received: 2 November 2020 / Accepted: 12 June 2021 / Published online: 11 August 2021

Abstract

Surface classification is an effective way to assess the surface quality of parts. During the last decade, the assessment of parts quality has gradually changed from simple geometries to complex three-dimensional (3D) surfaces. Traditional quality assessment methods rely on identifying key product characteristics of parts, e.g., the profile of surface. However, for point cloud data obtained by high-definition metrology, traditional methods cannot make full use of the data and lose a lot of information. This paper proposes a systematic approach for classifying the quality of 3D surfaces based on point cloud data. Firstly, point clouds of different samples are registered to the same coordinate system by point cloud registration. Secondly, the point cloud is divided into several sub-regions by fuzzy clustering. Finally, a novel parallel classification network method based on deep learning is proposed to directly process point cloud data and classify 3D surfaces. The performance of the proposed method is evaluated through simulation and an actual case study of the combustion chamber surfaces of the engine cylinder heads. The results show that the proposed method can significantly improve the classification accuracy of 3D surfaces based on point cloud data.

Keywords Three-dimensional surface · Quality classification · Point cloud data · Deep learning

Introduction

As manufacturing technologies advance, three-dimensional (3D) surfaces are increasingly being utilized for modern industrial applications. The quality of these surfaces has an important impact on the overall quality of products. For example, the inner surface of combustion chamber of engine cylinder head can greatly affect the performance of the engine, such as the compression ratio. Surface classification is one of the most effective means to identify surface quality and it is a critical process in product quality control.

Traditional quality control monitors the key product characteristics (KPCs) of manufactured parts, e.g., flatness (Wang et al., 2014a, 2014b; Zhang et al., 2016), roundness (Colosimo et al., 2008, 2010; Zhao et al., 2020) and surface profile (Jin et al., 2015). KPCs are collected and calculated by the measurement systems, such as caliper, coordinate measurement machine (CMM), or digital camera (Wells et al., 2021). However, with the recent advancement of measurement technology, high definition metrology (HDM) technologies, such as laser scanner, stereo camera and structured light system, have been gradually adopted for measurement. HDM collects millions of data points in seconds and its measurement accuracy can reach ± 1 μm (Wang et al., 2014a, 2014b). The measurement principle of HDM and an example of the measurement process of an engine block surface are shown in Fig. 1.

By contrast, traditional measurement methods only measure the points of interest and cannot fully reflect the entire contour of the surface. Figure 2 shows a comparison of

✉ Shichang Du
lovbin@sjtu.edu.cn

Chen Zhao
zhao_chen@sjtu.edu.cn

Jun Lv
jlv@dbm.ecnu.edu.cn

Yafei Deng
phoenixdyf@sjtu.edu.cn

Guilong Li
lgl52613@sjtu.edu.cn

[1] Department of Industrial Engineering and Management, School of Mechanical Engineering, Shanghai Jiao Tong University, Shanghai, China

[2] Faculty of Economics and Management, East China Normal University, Shanghai, China

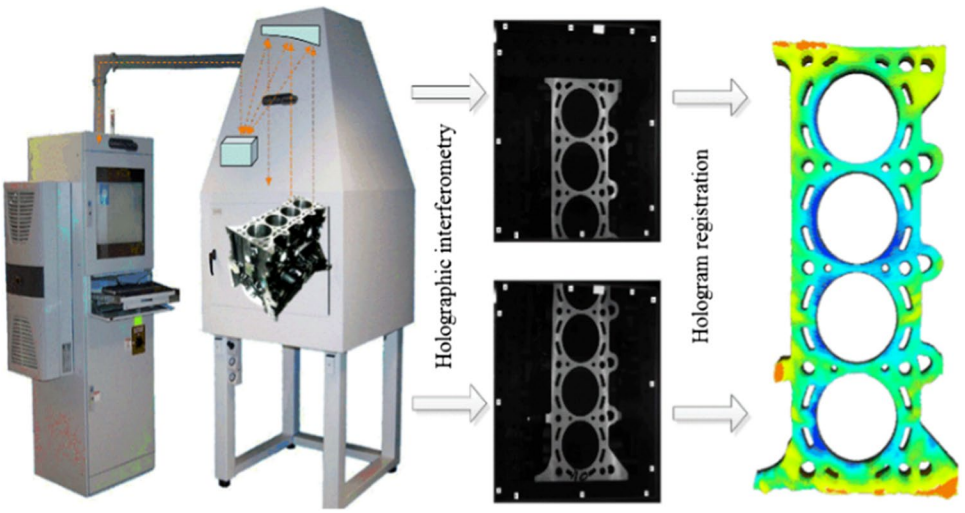

Fig. 1 Measurement by HDM

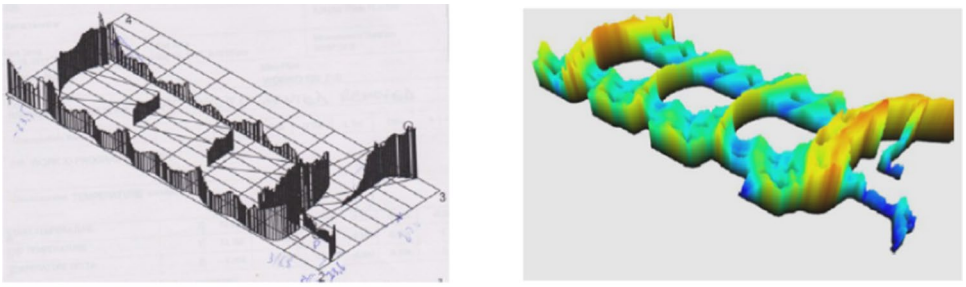

(a) CMM measurement result **(b)** HDM measurement result

Fig. 2 Comparison of different surface measurement techniques

CMM and HDM measurement techniques for measuring an engine block surface. Compared with CMM, the point cloud data collected by HDM can better reflect the complete 3D topography information of the entire surface.

For point cloud data, although KPCs can be used to detect related offsets, they do not make full use of all available information in the point cloud data. This mismatch between data and processing technology has caused the "rich data but poor information" problem (Choudhary et al., 2008). To date, several research studies have been conducted on profile monitoring and defects detection based on point cloud data. Du et al. (2015a, 2015b) proposed a series of point cloud filtering approaches based on support vector machine and shearlet methods, to extract different surface components. Wang et al. (2014a, 2014b) converted point cloud data into grayscale images to evaluate the form error of the surface. However, these researches only focus on planar surfaces.

Other proposed approaches suggest using control charts to monitor the deviation between the point cloud data and the nominal surface. Zang and Qiu (2018a, 2018b) calculated the translation and rotation matrix of the measurements and the nominal point cloud to monitor 3D printing surface quality. This method can be applied to an arbitrary 3D surface with regular and sparse measurements. Stankus and Castillo-Villar (2019) proposed a multivariate generalized likelihood ratio control chart to monitor a curved surface. Wells et al. (2021) converted the point cloud into a non-uniform rational basis spline (NURBS) model, and used the exponentially weighted moving average (EWMA) control chart to monitor the parameters of the NURBS model. However, these methods require a known nominal surface or a computer aided design (CAD) model, which are not available in some cases. Wang and Tsung (2005) and Wells et al. (2013) used a quantile–quantile (Q–Q) plot method to monitor point clouds. The Q-Q plot transforms high dimensional data into linear profiles to determine whether two sets of data come from the same distribution. Osada et al. (2002) and Laga et al. (2019) used distribution histogram to represent the shape characteristics of 3D surfaces. Huang et al. (2018) divided a 3D surface into small planes and then classified the surface based on the features of the small planes. Although these methods can be applied to assess the quality of 3D surfaces, using the feature extraction for complex 3D shapes may miss information about local changes.

To solve the problem that the existing methods have limited scenarios of application (difficult to apply to arbitrary 3D surface), this paper proposes a novel deep learning (DL) approach to process the point cloud data and

classify the quality of 3D surfaces which are composed of several sub-regions with different characteristics.

Recently, DL has emerged as a highly effective network structure for processing the high-density data. The multiple layers stacked in the network can fully capture the representative information from raw input data (Li et al., 2020). For point cloud data, recent advances of DL methods have mostly focused on object classification, such as the Volumetric-based method (Maturana & Scherer, 2015; Ning et al., 2020), multi-view method (Su et al., 2015; Wu et al., 2015), and PointNet method (Qi et al., 2016, 2017). To the best of our knowledge, no DL methods have been proposed for quality classification of 3D surfaces. Compared with object classification, quality classification of 3D surfaces requires more attention to the detailed characteristics of objects. This is important because the quality of some workpieces may be insufficient in a small area, and this variation may not be detected in an average evaluation of the entire shape.

In this paper, a systematic approach including a novel parallel classification network (PCN) is explored for the quality classification of 3D surfaces. In this approach, a 3D surface is registered and divided into several sub-regions. Based on DL, the features of the sub-regions are extracted and processed by the PCN to obtain the classification result of the 3D surface.

The rest of this paper is organized as follows. The framework and procedures of the proposed method are described in detail in "The proposed method" section. "Simulation study" section shows the simulation process, results and comparison with other methods. A real case about the inner surface quality classification of the engine cylinder head combustion chamber is discussed in "Case study" section. Concluding remarks are presented in "Conclusion" section.

The proposed method

Overview and framework

A 3D surface can be considered as the splicing of smooth and blending sub-regions. These sub-regions may have different characteristics due to the intended design or the processing method, so they make different contributions to the overall surface quality. In the proposed method, a 3D surface is segmented into several sub-regions according to the characteristics of the points. A novel neural network PCN including parallel neural network (PNN) and deep neural network (DNN) is designed to extract the features of sub-regions and classify the 3D surface.

The framework of the proposed approach is shown in Fig. 3, and the procedure involves the following steps.

Step 1: Region segmentation of 3D surface. In this step, a 3D surface is segmented into several sub-regions through point cloud registration and region segmentation. The normal vector and curvature are regarded as the characteristics of points, and are used to segment the surface region.

Step 2: Surface classification. The PCN method is developed to extract the features of sub-regions. PCN has two modules: PNN and DNN. For different sub-regions, the PNN is used to extract the features, and then the features are linearly combined and processed in the fully connected layers of DNN. The classification result is obtained by the output layer.

Region segmentation of 3D surface

Region segmentation is performed to divide a complex surface into individual sub-regions. Points with similar characteristics are considered as belonging to the same region. At the junction of two regions, the characteristics of points usually show great changes (Di Angelo & Di Stefano, 2015), so the points on different sides of the junction can be divided into various regions. The segmentation procedure involves point cloud registration and region segmentation, which are described in the following two subsections.

Point cloud registration

Point cloud registration is used to match the point clouds of all samples to the same coordinate system through rotation and translation transformation. In this stage, the principal component analysis (PCA) method is used to register the point clouds of different samples.

For a sample of point cloud data, first, the center point to the origin of the coordinate system is moved to obtain the translation matrix. Next, the principal component directions of the sample are calculated. The first three principal component directions are aligned with the X-axis, Y-axis, and Z-axis to obtain the rotation matrix. Last, the point cloud samples are aligned by the translation and rotation matrices. These procedures are performed on all point cloud samples. This unifies the coordinate systems and registers the point clouds of different samples.

Region segmentation

In modern product manufacturing processes, surface design is usually conducted via computer aided design/computer aided manufacturing (CAD/CAM). In CAD/CAM, product design involves various combinations of surfaces with different shapes. The actual processing or usage of these component surfaces differ, so there are different standards for quality evaluation with different effects on overall quality.

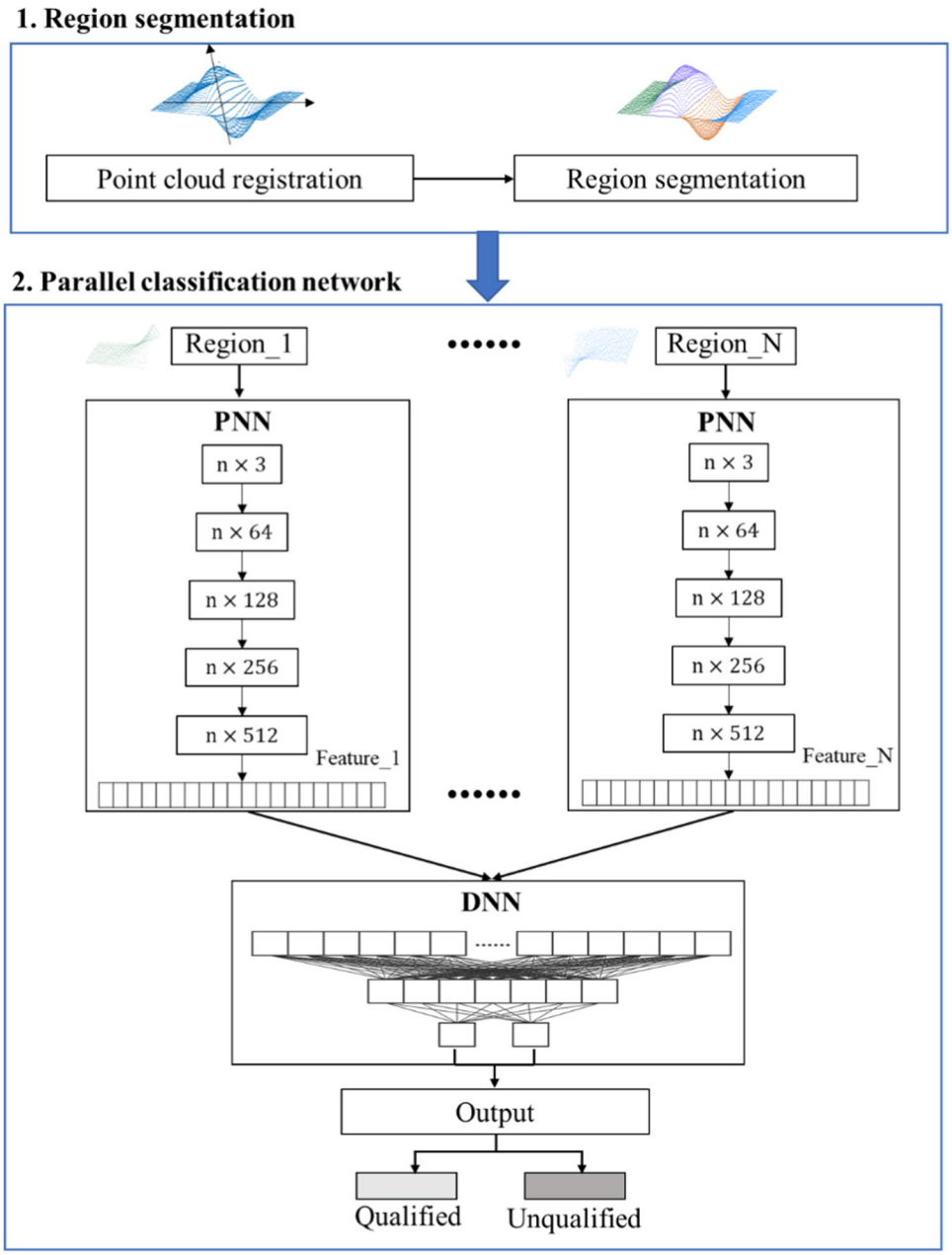

Fig. 3 Framework of the proposed method

Dividing the surface into meaningful natural point groups is essential for shape analysis and point cloud classification. Therefore, segmentation is a critical step in terms of point cloud processing.

For region segmentation, the measured point cloud data is divided into non-overlapping, single-characteristic connected regions based on the characteristic attributes of points. For classification based on deep learning, region segmentation reduces the disorder among points and assists the neural network to precisely extract the features of each sub-region.

Widely used methods of point cloud segmentation can be classified into three classes: edge-based, region-based and cluster-based methods (Nurunnabi et al., 2012). The first two methods are hard partitioned, unambiguous, and sensitive to noise. Fuzzy C-Means (FCM) clustering is used in this study to segment point cloud data. FCM clustering has strong robustness to noise because it uses an objective function to determine the degree of membership of each point belonging to a certain category.

In FCM algorithm, the point cloud data set $P = \{p_1, p_2, \ldots, p_n\}$ is divided into c subset, and each subset is represented by a $c \times n$ order matrix U. The objective function is defined as:

$$J_m(\mathrm{U},\mathrm{v}) = \sum_{i=1}^{n}\sum_{k=1}^{c}\left(\mu_{ik}\right)^m\left(d_{ik}\right)^2$$

where μ_{ik} is the membership value of the ith data in the kth category; m is the weighting parameter; d_{ik} is the feature weighted distance between the ith data p_i and the kth clustering center v_k, including the spatial distance, normal vector difference and curvature difference.

The optimal fuzzy partition is obtained by minimizing the objective function. It is operated in the following steps.

Step 1: Determine the number of clusters c, select the value of the parameter m, and initialize the cluster center V;

Step 2: Calculate or update membership matrix U, $\mu_{ik} = \left[\sum_{j=1}^{c}\left(\frac{d_{ik}}{d_{ij}}\right)^{\frac{2}{m-1}}\right]^{-1}$;

Step 3: Calculate or update new cluster centers V, $v_i = \frac{\sum_{i=1}^{n}(\mu_{ik})^m(d_{ik})^2}{\sum_{i=1}^{n}(\mu_{ik})^m}$;

Step 4: Repeat steps 2–3 until the distance between the new centroid and the original centroid is below a certain threshold.

In the FCM algorithm, the number of clusters is manually defined. When the composition of the object shape is relatively simple, or the object is composed of a small number of curved surfaces, the number of sub-regions can be intuitively defined manually. When the composition of the curved surface is too complicated to determine intuitively, the number of sub-regions can be determined by applying the elbow method. The elbow method consists of plotting the explained variation as a function of the number of clusters, then selecting the elbow of the curve as the number of clusters to use (Syakur et al., 2018).

Parallel classification network

After the region segmentation, the surface is divided into several sub-regions. The PCN is used to extract the features of the sub-regions and classify the 3D surface.

The structure of the classification network is shown in Fig. 4. It has two modules: PNN and DNN. The PNN is used to extract features of sub-regions by translating multidimensional arrays to vectors with reduced dimensions. In the DNN, the concatenated layer linearly connects the features of all sub-regions, and then the fully connected layers process the features and output the classification result.

Feature extraction based on PNN

Before the PNN, the points of each sub-region are resampled to ensure the same number of input points exists in the same region for each sample. This is important because in the neural network, the input data is processed in batches and the data vectors must be the same size. The farthest point sampling (FSP) method is used here to evenly sample the points in each region so that the number of points in the same region of different samples would be the same and that the points would be evenly distributed.

The structure of the PNN is shown in Table 1. The PNN has four convolutional layers and one pooling layer. In the convolution layers, the point cloud is convolved by one-dimensional (1D) convolution kernels. The size of the convolution kernels in each layer is shown in Table 1. For

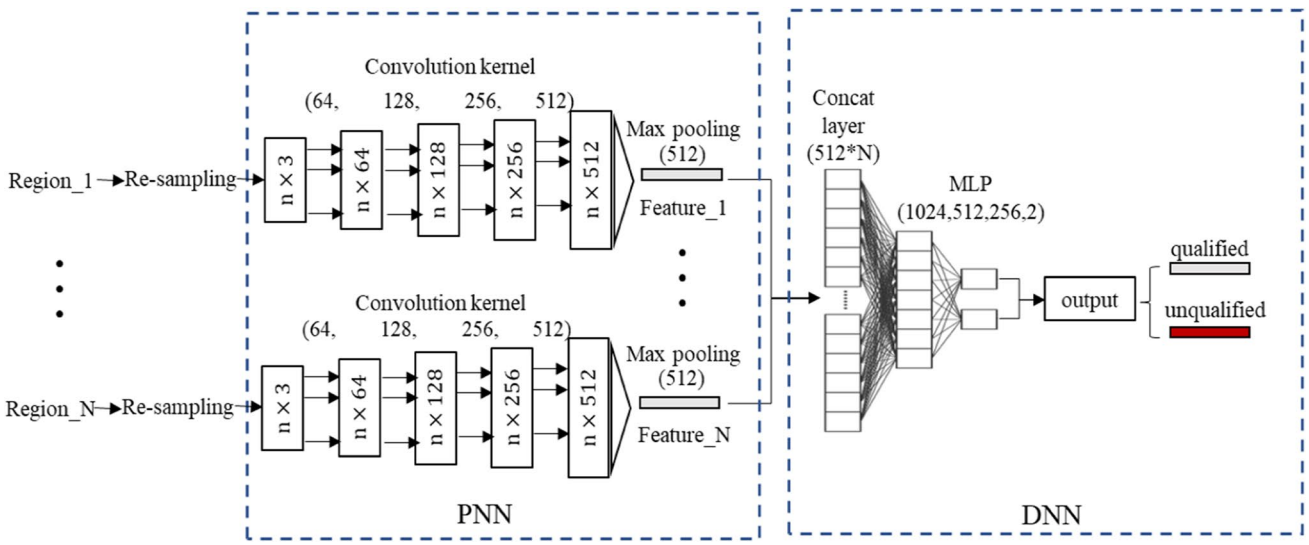

Fig. 4 The structure of the PCN

Table 1 The structure of the PNN

Parameter	L_1	L_2	L_3	L_4	Max pooling
Input	$n \times 3$	$n \times 64$	$n \times 128$	$n \times 256$	$n \times 512$
Conv	(3,64,1)	(64,128,1)	(128,256,1)	(256,512,1)	–
BatchNorm	64	128	256	512	–
Activation function	✓	✓	✓	–	–
Output	$n \times 64$	$n \times 128$	$n \times 256$	$n \times 512$	512

Table 2 The structure of the DNN

Parameter	L_1	L_2	L_3	L_4
Input	$N \times 512$	1024	512	256
Linear	($N \times 512$, 1024)	(1024, 512)	(512, 256)	(256, 2)
BatchNorm	1024	512	256	–
Activation function	✓	✓	✓	–
Dropout	✓	✓	✓	–
Output	1024	512	256	2

example, in the first layer, the dimension of the input data is $n \times 3$, where n is the number of the points of a sub-region. Each point is represented by a 3D coordinate value. The size of the convolution kernel is 3×1 and there are 64 convolution kernels, so the dimension of the output data is $n \times 64$. The data are then normalized and nonlinearized by BatchNorm and Activation function.

After four layers of convolution, a 512-dimensional feature is generated. The 3D features of each point are upgraded to 512 dimensions. A max pooling layer extracts 1D features by extracting the maximum values of the feature of points. The final output of the PNN is 512 features representing a sub-region.

Feature connection and classification based on DNN

DNN has a multi-layer structure and can reduce the dimension of the features through nonlinear transformation. In the DNN module, features obtained from N sub-regions are linearly connected by the concatenated layer and then the features are processed by the multi-layer perceptron (MLP). MLP is composed of several fully connected layers. These layers integrate the features and provide the output to the final classifier.

The structure of the DNN is shown in Table 2. The DNN has four linear layers. Each linear layer is fully connected, where each neuron is connected to all neurons in the previous layer. In the linear layer, the first number represents the number of input neurons and the latter number represents the number of output neurons. The output data are normalized and nonlinearized by BatchNorm and Activation function with a dropout to prevent overfitting. The last layer of the DNN outputs the classification result.

Simulation study

Problem description and analysis

In practical engineering applications, the surface of the product is usually composed of flat surfaces and natural quadric surfaces. A 3D surface consisting of cylindrical surface, spherical surface, and flat is designed for the purposes of this simulation accordingly. In this surface (Fig. 5), the random error of the designed qualified surface obeys the normal distribution: $\varepsilon \sim N(0, \sigma^2), \sigma^2 = 0.01$.

The four unqualified samples are designed as:

a. Global deviation, $\sigma^2 = 0.02, 0.03, 0.05$.
b. Deviation in the cylindrical surface, $\sigma^2 = 0.02, 0.03, 0.05$.
c. Deviation in the spherical surface, $\sigma^2 = 0.02, 0.03, 0.05$.
d. Deviation in the flat, $\sigma^2 = 0.02, 0.03, 0.05$.

These four deviation states are shown in Fig. 6.

After considering the different deviation states, the simulation contains the following four cases:

1. Case1. Training set and test set: $g_0(x)$ and $g_1(x)$.

   The unqualified samples of training set and test set are global deviation, and each deviation case (different σ^2 value) contains 20 samples. In this case, the number of samples in training set and test set are both 80.

2. Case 2. Training set: $g_0(x)$ and $g_1(x)$. Test set: $g_0(x)$, $g_2(x)$, $g_3(x)$ and $g_4(x)$.

   In the training set, the unqualified samples are global deviation. In the test set, the unqualified samples are local deviation. Each deviation case (different σ^2 value) contains 20 samples. In this case, the number of samples in training set and test set are 80 and 200 respectively.

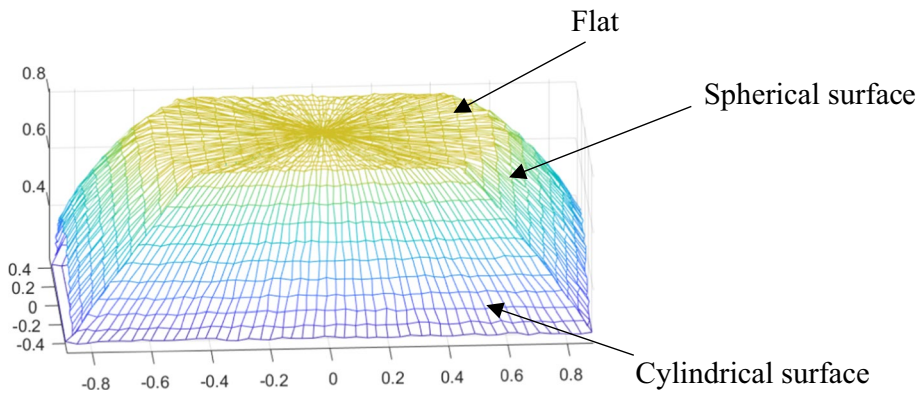

Fig. 5 The qualified surface $g_0(x)$

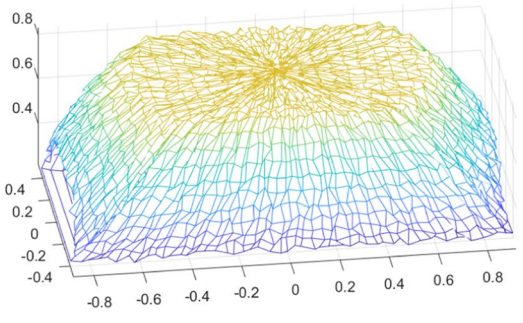

(a) Deviation in global space, $g_1(x)$

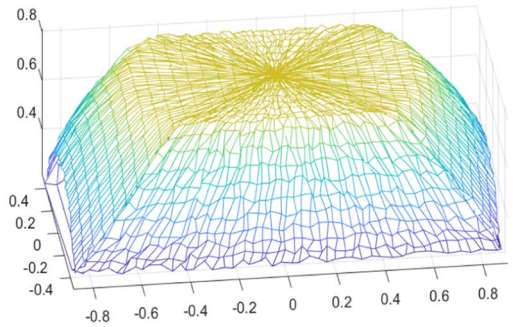

(b) Deviation in the cylindrical surface, $g_2(x)$

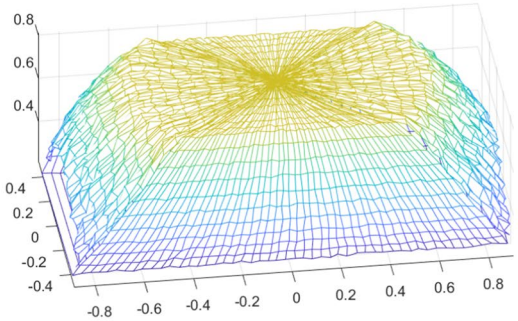

(c) Deviation in the spherical surface, $g_3(x)$

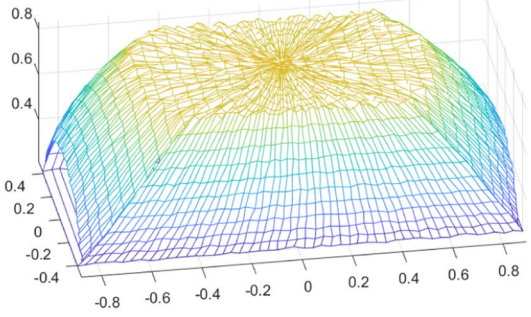

(d) Deviation in flat, $g_4(x)$

Fig. 6 The four deviation states

3. Case 3. Training set: $g_0(x)$, $g_2(x)$, $g_3(x)$ and $g_4(x)$. Test set: $g_0(x)$ and $g_1(x)$.

   In the training set, the unqualified samples are local deviation. In the test set, the unqualified samples are global deviation. Each deviation case (different σ^2 value) contains 20 samples. In this case, the number of samples in training set and test set are 200 and 80 respectively.
4. Case 4. Training set and test set: $g_0(x)$, $g_1(x)$, $g_2(x)$, $g_3(x)$ and $g_4(x)$.

The training set and test set samples contain all the conditions. the number of samples in training set and test set are both 260.

The simulated surface is composed of five continuous sub-surfaces. According to manual experience, five sub-regions provide effective segmentation results without over-segmentation. In the simulation, 1–6 sub-regions are segmented for comparison to verify this assertion. In addition, excessive sub-regions during point cloud segmentation result in different segmentation results of samples under high noise conditions. To eliminate this difference, the cluster

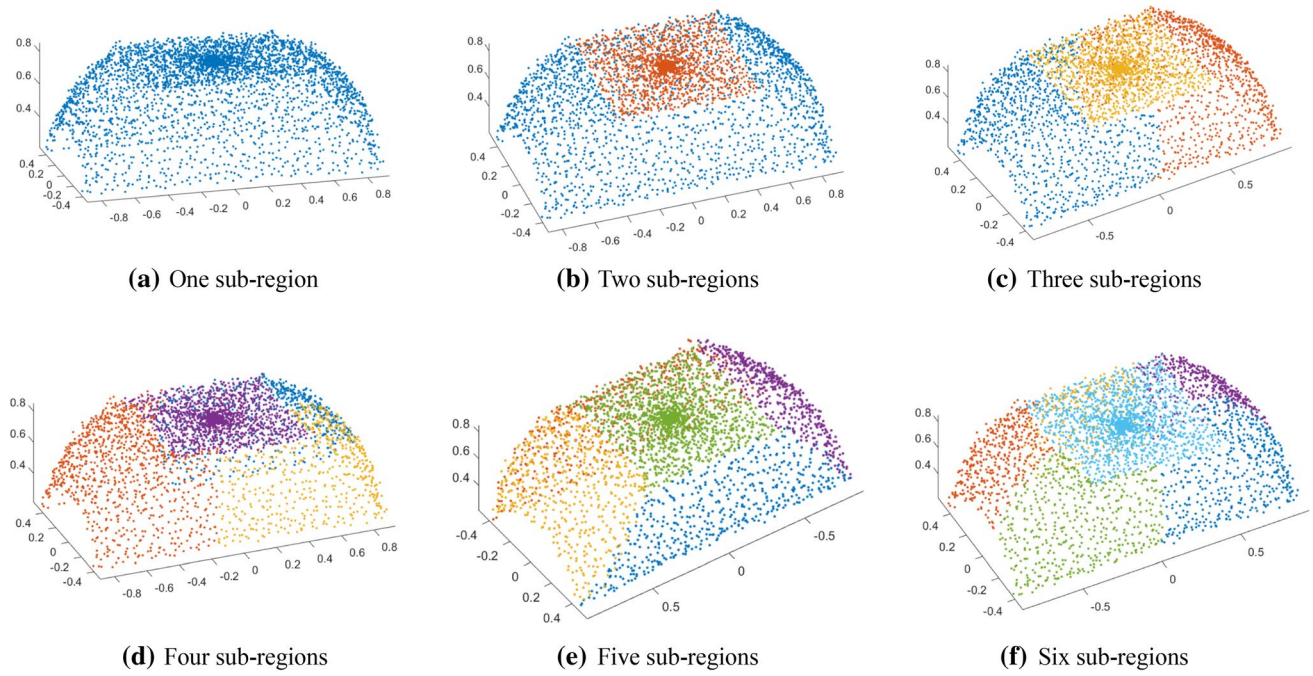

(a) One sub-region **(b)** Two sub-regions **(c)** Three sub-regions

(d) Four sub-regions **(e)** Five sub-regions **(f)** Six sub-regions

Fig. 7 Segmentation results under different numbers of sub-regions

Table 3 The values of hyperparameters in the PCN

Hyperparameter	Value
Dropout rate	0.3
Epoch	120
Learning rate	0.001
Activation function	Tanh

center matrix of the samples is saved in the training set to ensure that the locations of the regions in different samples are the same. Figure 7 shows the segmentation results under different numbers of sub-regions.

Hyperparameters in the classification network affect the learning process and final classification results. It is necessary to discuss the influence of the hyperparameters on the classification accuracy and the decrease rate of loss value. The values of hyperparameters determined by experiments can perform well in a variety of situations. Table 3 shows the hyperparameter values used in this study.

The classification accuracy of the PCN with 1–6 sub-regions and in various cases was determined respectively as shown in Table 4.

The number of sub-regions appears to significantly impact the classification results; additional sub-regions, further, are not necessarily preferable to fewer sub-regions. The case with five sub-regions shows highest classification accuracy. The simulation surface is composed of five sub-surfaces, so it follows that optimal results are achievable when the segmentation pattern mirrors the actual surface composition pattern. This conclusion is consistent with the theoretical assumption. Meaningful region segmentation can improve the accuracy of the classification network.

Table 4 The classification accuracy of PCN in simulation

Number of sub-regions	Case 1	Case 2	Case 3	Case 4	Average
1	0.767	0.589	0.731	0.664	0.688
2	0.875	0.701	0.845	0.762	0.796
3	0.913	0.706	0.874	0.787	0.820
4	0.924	0.712	0.866	0.801	0.826
5	**0.957**	**0.758**	**0.925**	**0.843**	**0.871**
6	0.936	0.720	0.872	0.819	0.837

The bold value indicates the optimal value in each case

The result also shows that Case 2 has the lowest classification accuracy. In Case 2, the partial deviation is tested by training the global deviation. Although the accuracy is not as strong in this case as in other cases, when the segmentation subregion is 5, the classification accuracy has been significantly improved. The results of Case 2 and Case 3 show that the proposed model has generalization ability.

As discussed below, the proposed method is also compared with other methods to further illustrate its effectiveness.

Comparison and discussion

There have been few studies on 3D surface quality classification based on point cloud data, especially methods based on deep learning. As PNN is used mainly for feature extraction, the approaches that extract features from point clouds are considered to be comparison. The existing feature extraction methods classify, evaluate, or monitor 3D surface according to the normal vector, curvature, and other descriptors of the point cloud. The descriptors express the geometric and topological properties of the shape of 3D surface, and they are divided into global and local features (Lara López et al., 2017). Global and local feature methods are described below with two representative methods given for comparison.

1. Global feature

The global feature is calculated from the information of all points in the point cloud. In this method, the geometric attributes can be described by a unique feature vector. Osada et al. (2002) first proposed measuring the geometric properties of a 3D model through a shape function. They calculated the probability of the shape function statistically, then used a distribution histogram to represent the shape characteristics. On this basis, Laga et al. (2019) estimated the dissimilarity between the two models by comparing their respective distribution histograms using dissimilarity measure. The χ^2 statistics are regarded as descriptors to represent this metric.

The application process of this method is as follows. First, calculate the histogram of the global features for each sample in the training set. Then, perform least squares fitting on the histograms of all qualified samples in the training set to obtain statistical distribution curve. In the test set, calculate the χ^2 statistics, i.e., the distance between the histogram of each sample and the distribution curve. When a statistic is greater than threshold, the corresponding sample is considered to be unqualified.

2. Local feature

Local features include statistics of vertex data, normal distribution, projection, and other factors related to the feature description of the vertex. A histogram or local geometric characteristic information statistics, such as normal and curvature and other features, are typically used to form feature descriptors. Huang et al. (2018) divided a 3D surface into multiple small areas, then approximated each small area to a plane. They explored wavelet packet entropy and normal vectors to represent the features of multiple small areas. They also proposed three individual control charts to monitor three quality parameters. If any quality parameter is out of control limit, the corresponding sample is considered to be unqualified.

These methods are well-established, effective methods for 3D surface classifying. The simulation results are shown in Table 5.

According to the results in Table 5, the proposed method has the highest classification accuracy in most cases, followed by the local feature method. The global feature method is the least effective of the three methods. The global feature method is not strong in discriminating details and easily loses the local features, so its inability to identify unqualified samples. Especially in Case 2 and Case 4, there are a large proportion of unqualified samples, the global feature method is almost impossible to classify correctly. The local feature method divides the surface into several small regions. Compared with the global feature method, it can extract more sufficient information. But because three control charts are used at the same time, it is easy to identify qualified samples as unqualified samples. Therefore, the local feature method has higher classification accuracy when the proportion of qualified products is relatively small.

The PCN instead divides the point cloud into meaningful sub-regions, then divides the point cloud manually to extract the feature information related to the deviation. The classification accuracy is significantly improved by the proposed method compared to the other methods, which further proves that the proposed method has strong generalization ability.

Case study

In this section, a case study on the inner surface quality classification of the engine cylinder head combustion chamber is analyzed to assess the application of the proposed method. The inner surface of the combustion chamber of the engine cylinder head is a 3D surface. The shape of the inner surface will affect the volume of the combustion chamber, which in turn affects the performance of the engine. The inner surface of the combustion chamber is made by casting. The mold is used under high temperature conditions and with frequent

Table 5 Comparison of classification accuracy

Method	Case 1	Case 2	Case 3	Case 4	Average
PCN	**0.957**	0.758	**0.925**	**0.843**	**0.871**
Global feature (Laga et al., 2019)	0.663	0.485	0.763	0.542	0.613
Local feature (Huang et al., 2018)	0.738	**0.775**	0.813	0.804	0.783

The bold value indicates the optimal value in each case

contact with the casting material for a long period of time, which can lead to wear.

In the current production, the quality of the inner surface is indirectly determined by mold inspection by the CMM. In the mold inspection, the measurement area and the number of measurement points are artificially selected, and the quality of the mold is evaluated by using engineering experience. This method can only measure the mold at intervals, which can easily miss problems in batches of parts, resulting in major losses.

By using HDM, the point cloud data of the inner surface can be obtained within minutes, and the inner surface can be directly measured. Therefore, any errors in the processing of the cylinder head combustion chamber can be rapidly identified by analyzing the inner surface point cloud data, allowing the quick adjustment of the mold as needed to ensure product quality.

In this experiment, sixteen B12 series engines of an automobile processing plant are measured by HDM equipment to obtain the point cloud data of cylinder head combustion chambers. Figure 8 shows the measurement process of the cylinder head. Figure 8a is the measurement equipment, and Fig. 8b is the measurement process. The cylinder heads are scanned from left to right by line laser. Each line of the line laser contains 1280 points, and 2000–3000 lines are measured for each cylinder head. Figure 9 shows the point cloud data of an engine cylinder head. Figure 10 shows the point cloud data of one cavity.

Result analysis

A total of 64 combustion chambers are measured by HDM equipment, including 24 unqualified samples which are manually tested due to mold wear. These samples are equally distributed to the training set and test set.

After measuring the point cloud, there are approximately 90,000 points in each cavity, and the number of sampling points is abundant. In order to expand the training set, 70,000 points are taken for each sample at random. Each point cloud is sampled twice to double the training set. Therefore, there are 64 samples in the training set and 32 samples in the test set.

Consider a sample cavity as an example of the preprocessing and segmentation processes of combustion chambers. During measurement, the interference of ambient light and the surface reflection of the measured workpiece will produce outliers. Because the point cloud obtained by HDM is high-density and the outliers are prominent and easily detected, the outliers can be eliminated by using the spatial distance from the neighbor points of the point cloud (Huang et al., 2018). The average distance of the K-nearest neighbor points of each point is calculated first. Then the 3σ law is used to eliminate outliers. When an average distance of a point is larger than the total limit, the point is considered an outlier and should be eliminated. As shown in Fig. 11, the points in the red circle are outliers and need to be eliminated.

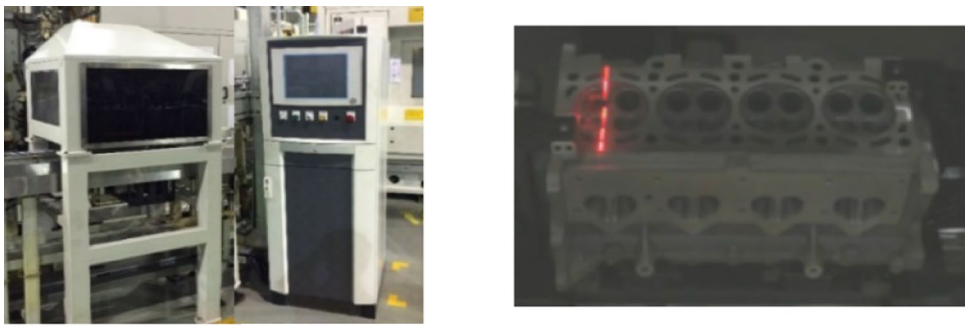

(a) HDM equipment **(b)** Line laser measurement process

Fig. 8 The measurement process of cylinder head

(a) An engine cylinder head **(b)** Point cloud data of an engine cylinder head

Fig. 9 Point cloud data of an engine cylinder head

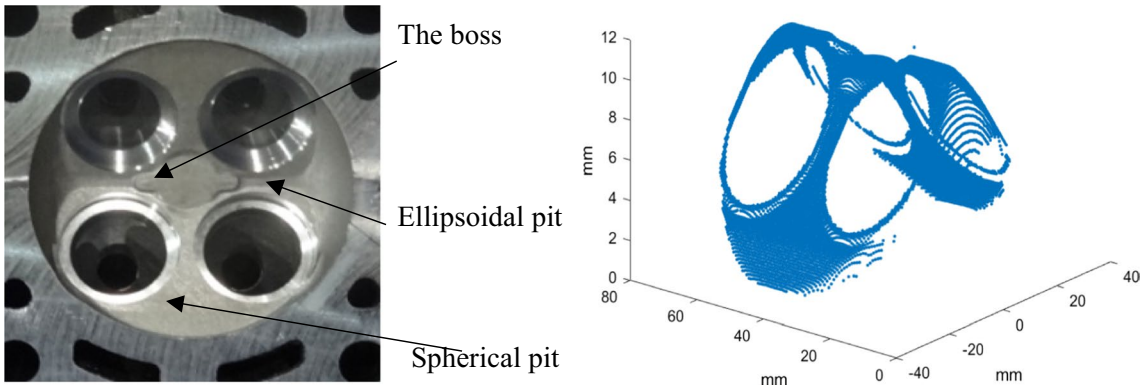

(a) A cavity of engine cylinder head **(b)** Point cloud data of a cavity

Fig. 10 Point cloud data of a cavity of engine cylinder head

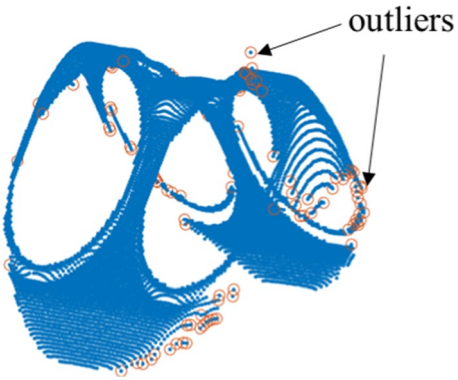

Fig.11 The outliers of the point cloud

Fig.13 The sub-region division of the point cloud

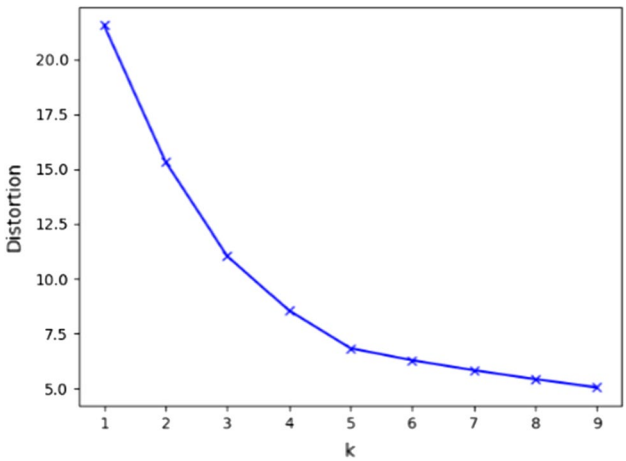

Fig. 12 The elbow curve of the number of sub-regions

Similar to the simulation surface, the cavity is composed of three different surface types. The elbow method is used here to determine the number of sub-regions of the combustion chamber surface. As shown in Fig. 12, when the number of sub-regions is 5, the curve reaches the inflection point. The number of sub-regions is set to five to obtain the segmentation results shown in Fig. 13.

Each sample is sampled, registered, and segmented according to the proposed method, then trained and tested using the PCN. Figure 14 shows the process of training and test. The final accuracy of the test set is 0.848.

Comparison and discussion

The same training and test sets are used to compare PCN with global feature and local feature methods. The results are shown in Table 6.

Table 6 shows that the proposed method has the highest classification accuracy, followed by the local feature method. Global feature method shows the lowest accuracy. These

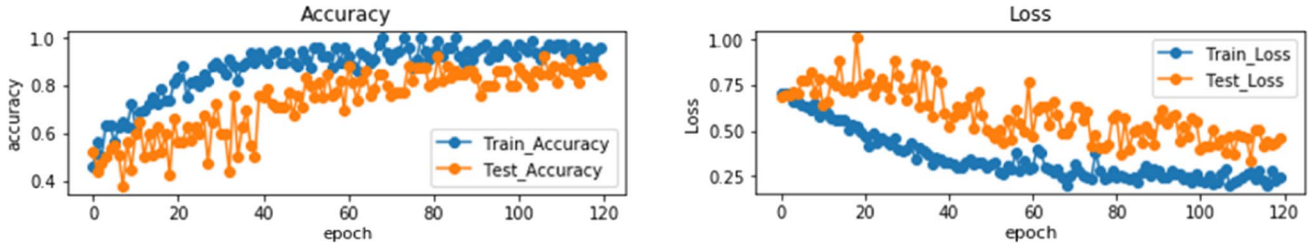

Fig.14 The classification result of the proposed method

Table 6 The classification results of the methods

Method	Accuracy
PCN	**0.848**
Global feature (Laga et al., 2019)	0.625
Local feature (Huang et al., 2018)	0.781

The bold value indicates the optimal value

results are consistent with simulation results. The proposed method is 6.7% and 22.3% more accurate than the global feature and local feature methods, respectively. For complex cylinder head surfaces, the proposed method remains good performance.

Conclusion

The PCN method is established in this study based on deep learning for the quality classification of 3D surfaces. This method is the first to apply deep learning to point cloud-based surface quality classification. This method includes region segmentation and quality classification. In region segmentation, the points with similar features are divided into the same region. In quality classification, a novel network PCN is proposed to directly extract the features of point cloud data and classify 3D surfaces.

Compared with the two representative point cloud feature extraction methods, the proposed method shows promising results in both simulations and the case study. In the simulation, different training and test sets are constructed for comparison. Simulation results show that meaningful point cloud segmentation positively affects the feature extraction of neural networks. From the method comparison results, the proposed PCN shows the highest classification accuracy in most cases, suggesting that it has strong generalization ability. In the case study, the inner surface quality of the engine cylinder head combustion chamber is classified to further test the proposed method. Compared with other methods, the proposed method exhibits a significantly higher classification accuracy. Taken together, the results show that the use of segmentation and feature extraction for sub-regions markedly improves the overall classification effect. The processing of detailed information appears to remit better 3D surface quality classification results than global information processing. Moreover, the results of automatic extraction of sub-region features through neural networks are better than artificial local features.

The results indicate that the proposed method is suitable for classifying 3D surfaces based on point cloud data. Large amounts of data can be obtained in the production line, leading to further improvement of the classification results. There are several possible directions for future research.

1. In this study, only offline data is used to classify the surface quality. The accuracy and stability of the algorithm should be improved for use with online detection. Combined with the rapid measurement of HDM equipment, this method can be used to quickly detect changes in production conditions that alter surface quality, and realize the online classification of 3D surface quality.
2. The use of 3D point cloud data is a significant research challenge. This method provides a reference for the detailed information extraction of high-density point cloud data and can be combined with other point cloud technologies for accurate and rapid processing of point cloud data.

Acknowledgements The authors greatly acknowledge the editor and the reviewers for their valuable comments and suggestions that have led to a substantial improvement of the paper. This work was supported by the National Natural Science Foundation of China (Grant No. 51775343) and the Shanghai Pujiang Program (Grant No. 18PJC031).

References

Choudhary, A. K., Harding, J. A., & Tiwari, M. K. (2008). Data mining in manufacturing: A review based on the kind of knowledge. *Journal of Intelligent Manufacturing, 20*(5), 501. https://doi.org/10.1007/s10845-008-0145-x

Colosimo, B. M., Mammarella, F., & Petrò, S. (2010). Quality control of manufactured surfaces. *Frontiers in Statistical Quality Control, 9*, 55–70.

Colosimo, B. M., Semeraro, Q., & Pacella, M. (2008). Statistical process control for geometric specifications: On the monitoring of roundness profiles. *Journal of Quality Technology, 40*(1), 1–18. https://doi.org/10.1080/00224065.2008.11917709

Di Angelo, L., & Di Stefano, P. (2015). Geometric segmentation of 3D scanned surfaces. *Computer-Aided Design, 62*, 44–56. https://doi.org/10.1016/j.cad.2014.09.006

Du, S., Liu, C., & Huang, D. (2015a). A shearlet-based separation method of 3D engineering surface using high definition metrology. *Precision Engineering, 40*, 55–73. https://doi.org/10.1016/j.precisioneng.2014.10.004

Du, S., Liu, C., & Xi, L. (2015b). A selective multiclass support vector machine ensemble classifier for engineering surface classification using high definition metrology. *Journal of Manufacturing Science and Engineering, 137*(1), 011003. https://doi.org/10.1115/1.4028165

Huang, D., Du, S., Li, G., Zhao, C., & Deng, Y. (2018). Detection and monitoring of defects on three-dimensional curved surfaces based on high-density point cloud data. *Precision Engineering, 53*, 79–95. https://doi.org/10.1016/j.precisioneng.2018.03.001

Jin, Y.-A., Li, H., He, Y., & Fu, J.-Z. (2015). Quantitative analysis of surface profile in fused deposition modelling. *Additive Manufacturing, 8*, 142–148. https://doi.org/10.1016/j.addma.2015.10.001

Laga, H., Guo, Y., Tabia, H., Fisher, R. B., & Bennamoun, M. (2019). Global shape descriptors. In *3D shape analysis* (pp. 65–91). John Wiley & Sons, Ltd.

Lara López, G., Peña Pérez Negrón, A., Antonio Jiménez, A., Ramírez Rodríguez, J., & Imbert Paredes, R. (2017). Comparative analysis of shape descriptors for 3D objects. *Multimedia Tools and Applications, 76*(5), 6993–7040. https://doi.org/10.1007/s11042-016-3330-5

Li, X., Zhang, W., Ding, Q., & Sun, J.-Q. (2020). Intelligent rotating machinery fault diagnosis based on deep learning using data augmentation. *Journal of Intelligent Manufacturing, 31*(2), 433–452. https://doi.org/10.1007/s10845-018-1456-1

Maturana, D., & Scherer, S. (2015). VoxNet: A 3D convolutional neural network for real-time object recognition. In *IEEE/RSJ international conference on intelligent robots and systems (IROS)*, 28 Sept–2 Oct 2015 (pp. 922–928). https://doi.org/10.1109/IROS.2015.7353481.

Ning, F., Shi, Y., Cai, M., & Xu, W. (2020). Various realization methods of machine-part classification based on deep learning. *Journal of Intelligent Manufacturing, 31*(8), 2019–2032. https://doi.org/10.1007/s10845-020-01550-9

Nurunnabi, A., Belton, D., & West, G. (2012). Robust segmentation in laser scanning 3D point cloud data. In *International conference on digital image computing techniques and applications (DICTA)*, 3–5 Dec 2012 (pp. 1–8). https://doi.org/10.1109/DICTA.2012.6411672.

Osada, R., Funkhouser, T., Chazelle, B., & Dobkin, D. (2002). Shape distributions. *ACM Transactions on Graphics, 21*(4), 807–832. https://doi.org/10.1145/571647.571648

Qi, C. R., Su, H., Mo, K., & Guibas, L. J. (2016). PointNet: Deep learning on point sets for 3D classification and segmentation. In *IEEE 2017 conference on computer vision and pattern recognition (CVPR)*, 21–26 July 2017 (pp. 652–660). arXiv:1612.00593.

Qi, C. R., Yi, L., Su, H., & Guibas, L. J. (2017). PointNet++: Deep hierarchical feature learning on point sets in a metric space. In *31nd Conference on neural information processing systems (NeurIPS)*, 4–9 Dec 2017 (pp. 5105–5114). arXiv:1706.02413.

Stankus, S. E., & Castillo-Villar, K. K. (2019). An improved multivariate generalised likelihood ratio control chart for the monitoring of point clouds from 3D laser scanners. *International Journal of Production Research, 57*(8), 2344–2355. https://doi.org/10.1080/00207543.2018.1518600

Su, H., Maji, S., Kalogerakis, E., & Learned-Miller, E. (2015). Multi-view convolutional neural networks for 3D shape recognition. In *IEEE international conference on computer vision (ICCV)*, 13–16 Dec 2015 (pp. 945–953). https://doi.org/10.1109/ICCV.2015.114.

Syakur, M. A., Khotimah, B. K., Rochman, E., & Satoto, B. D. (2018). Integration k-means clustering method and elbow method for identification of the best customer profile cluster. *IOP Conference Series: Materials Science and Engineering, 336*, 012017. https://doi.org/10.1088/1757-899X/336/1/012017

Wang, A., Wang, K., & Tsung, F. (2014a). Statistical surface monitoring by spatial-structure modeling. *Journal of Quality Technology, 46*(4), 359–376. https://doi.org/10.1080/00224065.2014.11917977

Wang, K., & Tsung, F. (2005). Using profile monitoring techniques for a data-rich environment with huge sample size. *Quality and Reliability Engineering International, 21*(7), 677–688. https://doi.org/10.1002/qre.711

Wang, M., Xi, L., & Du, S. (2014b). 3D surface form error evaluation using high definition metrology. *Precision Engineering, 38*(1), 230–236. https://doi.org/10.1016/j.precisioneng.2013.08.008

Wells, L. J., Dastoorian, R., & Camelio, J. A. (2021). A novel NURBS surface approach to statistically monitor manufacturing processes with point cloud data (Report). *Journal of Intelligent Manufacturing, 32*(2), 329. https://doi.org/10.1007/s10845-020-01574-1

Wells, L., Megahed, F., Niziolek, C., Camelio, J., & Woodall, W. (2013). Statistical process monitoring approach for high-density point clouds. *Journal of Intelligent Manufacturing, 24*(6), 1267–1279. https://doi.org/10.1007/s10845-012-0665-2

Wu, Z., Song, S., Khosla, A., Yu, F., Zhang, L., Tang, X., et al. (2015). 3D ShapeNets: A deep representation for volumetric shapes. In *IEEE conference on computer vision and pattern recognition (CVPR)*, 7–12 June 2015 (pp. 1912–1920). https://doi.org/10.1109/CVPR.2015.7298801.

Zang, Y., & Qiu, P. (2018a). Phase I monitoring of spatial surface data from 3D printing. *Technometrics, 60*(2), 169–180. https://doi.org/10.1080/00401706.2017.1321585

Zang, Y., & Qiu, P. (2018b). Phase II monitoring of free-form surfaces: An application to 3D printing. *Journal of Quality Technology, 50*(4), 379–390. https://doi.org/10.1080/00224065.2018.1508274

Zhang, L., Wang, K., & Chen, N. (2016). Monitoring wafers' geometric quality using an additive Gaussian process model. *IIE Transactions, 48*(1), 1–15. https://doi.org/10.1080/0740817X.2015.1027455

Zhao, C., Du, S., Deng, Y., Li, G., & Huang, D. (2020). Circular and cylindrical profile monitoring considering spatial correlations. *Journal of Manufacturing Systems, 54*, 35–49. https://doi.org/10.1016/j.jmsy.2019.11.011